Cell–cell contact globally activates microRNA biogenesis

Hun-Way Hwang[a], Erik A. Wentzel[b], and Joshua T. Mendell[a,b,c,d,1]

[a]Program in Human Genetics and Molecular Biology, [b]McKusick–Nathans Institute of Genetic Medicine, [c]Department of Pediatrics, and [d]Department of Molecular Biology and Genetics, Johns Hopkins University School of Medicine, Baltimore, MD 21205

MicroRNAs (miRNAs) are 18- to 24-nt RNA molecules that regulate messenger RNAs (mRNAs). Posttranscriptional mechanisms regulate miRNA abundance during development as well as in cancer cells where miRNAs frequently exhibit dysregulated expression. The molecular mechanisms that govern the global efficiency of miRNA biogenesis in these settings remain incompletely understood, and experimental systems for the biochemical dissection of these pathways are currently lacking. Here, we demonstrate that miRNAs are subject to dynamic posttranscriptional regulation in widely used cell culture systems. As diverse mammalian and *Drosophila* cell lines are grown to increasing density, miRNA biogenesis is globally activated, leading to elevated mature miRNA levels and stronger repression of target constructs. This broad increase in miRNA abundance is associated with enhanced processing of miRNAs by Drosha and more efficient formation of RNA-induced silencing complexes. These findings uncover a critical parameter necessary for accurate analysis of miRNAs in cell culture settings, establish a tractable system for the study of regulated miRNA biogenesis, and may provide insight into mechanisms that influence miRNA expression in physiologic and pathophysiologic states.

Drosha | RNA-induced silencing complex

MicroRNAs (miRNAs) are a diverse class of 18- to 24-nt RNA molecules that broadly impact cellular gene expression programs by regulating the stability and translational efficiency of messenger RNAs (mRNAs) (1, 2). miRNAs are first transcribed by RNA polymerase II as long primary transcripts (pri-miRNAs) that are capped, polyadenylated, and frequently spliced (3). Within these transcripts, sequences containing the miRNA form ≈60- to 80-nt hairpin structures that are excised by the Drosha–DGCR8 complex and transported out of the nucleus by exportin 5. In the cytoplasm, these hairpin structures, known as pre-miRNAs, undergo further processing by the Dicer–TRBP complex to produce a fully processed RNA duplex. One strand of this duplex, destined to become the mature miRNA, selectively associates with a member of the Argonaute (Ago) family of proteins. The miRNA, Ago protein, and additional associated proteins, collectively referred to as the RNA-induced silencing complex (RISC), interact with target mRNAs that are subsequently translationally repressed or degraded (4).

In animals, miRNAs provide functions essential for normal development and cellular homeostasis, and accordingly, their dysfunction has been linked to several human diseases (5, 6). A large fraction of miRNAs exhibit strict developmental stage-specific and tissue-specific expression patterns that are critical for their appropriate activity (7, 8). Although control of miRNA transcription plays an important role in shaping these expression patterns (9, 10), recent data have uncovered a significant role for posttranscriptional mechanisms of miRNA regulation. For example, in embryonic stem cells and during early mammalian development, the Lin-28 RNA-binding protein inhibits biogenesis of the let-7 family of miRNAs by binding to the loop regions of these pre-miRNAs (11–15). Nuclear sequestration of pre-miR-31 prevents its processing by Dicer in several human cancer cell lines (16) whereas pre-miR-138 is exported to the cytoplasm

but its cleavage by Dicer is inhibited by an unidentified factor in a variety of mouse tissues (17). In addition to these miRNA-specific mechanisms, the global efficiency of miRNA biogenesis is subject to regulation in some settings. For instance, during early development, inefficient maturation prevents the conversion of many abundant pri-miRNAs into mature miRNAs (18). Similarly, in many human cancers, reduced processing contributes to widespread down-regulation of miRNA expression (18–20). This inefficient processing of miRNAs in cancer cells has been demonstrated to promote tumorigenesis in both in vitro and in vivo models (21). The molecular mechanisms that control the global efficiency of miRNA biogenesis in these settings remain uncharacterized, and tractable experimental systems for the biochemical dissection of miRNA processing complexes under these conditions are currently lacking.

In this study, we set out to investigate the role of miRNAs in contact inhibition, the potent arrest of cellular proliferation that occurs after cell–cell contact. Unexpectedly, in both nontransformed cell lines that exhibit contact inhibition and in cancer cell lines that continue proliferating after contact, we observed up-regulation of the majority of expressed miRNAs as cells were grown to increasing density. This broad increase in miRNA abundance is associated with globally enhanced processing of miRNA primary transcripts by the Drosha endonuclease and more efficient incorporation of miRNAs into RISC. These findings reveal a previously unidentified link between cell–cell contact and miRNA expression, establishing a tractable system to study the global regulation of miRNA biogenesis and providing insight into mechanisms that shape miRNA expression patterns during development and in disease.

Results

Widespread Increase in miRNA Aundance with Increasing Cell Density. Loss of contact inhibition is a hallmark of cancer cells (22). To investigate whether specific miRNAs participate in this response, we profiled miRNA expression in subconfluent and confluent cultures of primary human fibroblasts and immortalized murine fibroblasts (NIH 3T3 cells), cell lines that undergo a well-characterized proliferation arrest upon cell–cell contact (23). As a control, we also examined miRNA expression under identical conditions in HeLa cells, a cancer cell line that does not exhibit contact inhibition (24). Unexpectedly, in all 3 cell lines, we observed a widespread increase in miRNA abundance in confluent cultures. The majority of expressed miRNAs were induced at confluence in fibroblasts and NIH 3T3 cells (1.25-fold to >10-fold), and nearly half of expressed miRNAs in HeLa cells

Fig. 1. Widespread up-regulation of miRNA expression in confluent cells. (*A*) Scatter plots showing miRNA expression in confluent versus subconfluent primary fibroblast, NIH 3T3, and HeLa cell lines. miRNAs that were detectable in both conditions are plotted. (*B*) Northern blots demonstrating miRNA abundance in HeLa cells at increasing levels of confluency. Representative images of U6 snRNA and ethidium bromide staining are shown. For this and subsequent figures, numbers below blots represent relative abundance of each miRNA normalized to U6 expression. (*C*) miRNA expression 24 h after plating HeLa and NIH 3T3 cells at increasing density. (*D*) Relative firefly luciferase activity derived from 3′ UTR reporter constructs containing sites of complete (perfect) or partial (bulged) complementarity to miR-15a or miR-143 after transfection into subconfluent or confluent HeLa cells. Values were normalized to luciferase activity produced from a reporter plasmid lacking miRNA-binding sites (pGL3-control) under each condition. Renilla luciferase activity produced from a cotransfected plasmid controlled for differences in transfection efficiency. Error bars represent standard deviations from 3 independent measurements. Representative data from 3 independent experimental trials, all of which yielded similar results, are shown.

responded in a similar manner [Fig. 1*A* and supporting information (SI) Tables S1–S3]. In contrast, the expression of very few miRNAs decreased in confluent cells.

To validate these findings, cells were grown to increasing density, with daily media replenishment to avoid confounding effects from depletion of nutrients, and miRNA abundance was examined by Northern blot analysis. These results closely paralleled the array data, with 11 of 13 examined miRNAs exhibiting a 1.5- to 8-fold induction (4.5-fold mean increase) in HeLa cultures grown to increasing density (Fig. 1*B*). Importantly, the abundance of U6 snRNA, 5S rRNA, and 5.8S rRNA was unchanged with increasing confluency, indicating that RNA isolated from high-density cultures was not artifactually overloaded. Similar results were obtained with a more limited set of miRNAs in primary fibroblasts and NIH 3T3 cells (Fig. S1*A*). Increased miRNA levels could also be induced rapidly by plating cells at escalating density and harvesting within 24 h (Fig. 1*C*). Notably, in many cases where pre-miRNAs were detectable by Northern blot analysis, they exhibited higher abundance with increasing cell density as well (Fig. S1*B*).

To assess whether miRNAs that accumulate in high-density cultures are actively incorporated into the RISC, we constructed reporter constructs with multiple sites of complete or partial complementarity to miR-15a or miR-143 in the 3′ UTR of luciferase. Greater repression of luciferase activity was observed when each construct was introduced into confluent cultures compared with subconfluent cultures (Fig. 1*D*), demonstrating that the accumulating miRNAs are functionally active.

miRNA Abundance Is Linked to Cell Density in Diverse Mammalian and *Drosophila* Cell Lines. The observation that primary fibroblasts, NIH 3T3, and HeLa cells grown to increasing density all exhibit widespread miRNA up-regulation despite their diverse ontogeny and differential ability to undergo contact inhibition suggests that this may be a widespread phenomenon. We therefore examined miRNA expression in subconfluent and confluent cultures of 5 additional commonly used human and mouse cell lines with diverse tissues of origin (MCF7, human breast carcinoma; HCT116, human colorectal carcinoma; MiaPaCa-2, human pancreatic adenocarcinoma; Hepa1–6, mouse hepatocellular carcinoma; and HEK293, human embryonic kidney). Increased abundance of miRNAs at confluence was observed for all tested cell lines with the exception of HEK293, in which only 2 of 5 miRNAs tested showed >1.5-fold
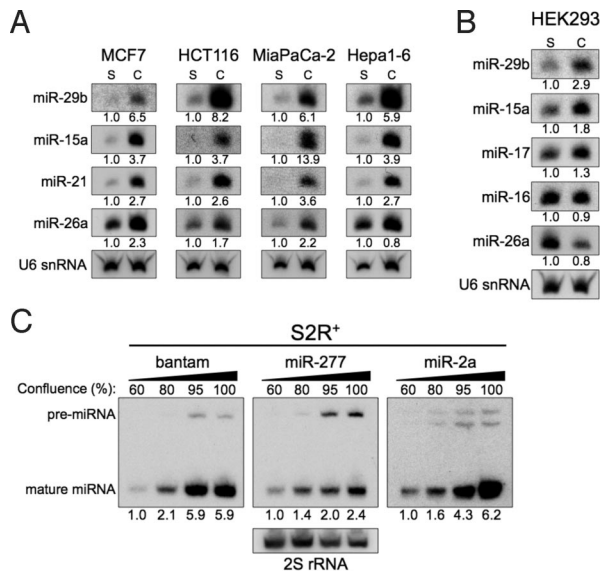
CELL BIOLOGY

Fig. 2. Globally increased miRNA abundance in confluent cultures of diverse animal cell lines. (*A*) Northern blots demonstrating miRNA abundance in subconfluent (S) and confluent (C) human and mouse cell lines. (*B*) Limited miRNA accumulation in confluent HEK293 cells. (*C*) Up-regulation of both precursor and mature miRNAs in *Drosophila* S2R+ cells at increasing confluency. 2S rRNA served as a loading control.

up-regulation under these conditions (Fig. 2 *A* and *B*). To determine whether this phenomenon is restricted to mammalian cells, we cultured *Drosophila* S2R+ cells, which have been widely used for miRNA studies. As observed for human and mouse cell lines, a dramatic increase in the abundance of both pre-miRNAs and mature miRNAs was observed with increasing cell density (Fig. 2*C*). These data document that miRNA abundance is linked to cell density in widespread animal cell lines and is an ancient response, likely present in a common ancestor of mammals and insects.

Establishment of Stable Cell–Cell Contacts Likely Triggers the Increase in miRNA Abundance. The observed up-regulation of miRNAs could be triggered by one of several possible events occurring when cells are grown to increasing density. These include reduced proliferation or quiescence of cells in confluent monolayers, release of diffusible factors that initiate the response, or establishment of stable cell–cell contacts. Several experiments were performed to distinguish between these possibilities. First, we assessed whether miRNA abundance correlates with proliferation rate or cellular quiescence. HeLa cells were monitored over a prolonged time course, beginning before and extending several days beyond confluence. Increased miRNA levels were observed shortly after cells reached confluence despite no measurable slowing of proliferation (Fig. 3*A*). Additionally, we documented that miRNAs are not increased in subconfluent primary fibroblasts and NIH 3T3 cells arrested by serum starvation (Fig. 3*B*). These observations indicate that global miRNA induction does not occur as a consequence of reduced cellular proliferation or cellular quiescence. This response is also unlikely to be induced by diffusible factors released in high-density cell cultures because subconfluent HeLa cells grown for 24 h in media conditioned by confluent cells did not exhibit increased miRNA levels (Fig. 3*C*). Together, these findings are most consistent with the establishment of cell–cell contacts as the initiating event that induces the global increase in miRNA abundance. A prediction of this model is that suspension cells that do not establish extensive stable cell–cell interactions will not show increased miRNA levels upon growth to high density.

Indeed, culture of the Ramos lymphoma cell line and the K562 leukemia cell line at increasing density does not significantly influence miRNA abundance (Fig. 3*D*).

Accumulation of miRNAs with Increasing Cell Density Occurs Through a Posttranscriptional Mechanism. Biogenesis of animal miRNAs initiates with transcription by RNA polymerase II, proceeds through 2 sequential processing events by the RNase III endonucleases Drosha and Dicer, and concludes with final loading of the mature miRNA into an Ago protein within RISC (3). To address whether accumulation of miRNAs is the result of an increase in transcription, we used quantitative PCR (qPCR) to measure the abundance of an extensive panel of primary transcripts that encode miRNAs that are robustly induced with increasing cell density (Figs. 1*B* and 4*A*). The levels of 9 of 10 primary transcripts were either unchanged or reduced with increasing confluency in HeLa cells. The sole exception was the primary transcript encoding miR-34a, which was dramatically up-regulated upon confluence, perhaps reflecting the known role of this miRNA in cellular senescence programs (25). Similar results were obtained in primary fibroblasts with 7 of 8 primary miRNA transcripts showing unchanged or decreased abundance at confluence (Fig. S2). These results indicate that miRNA primary transcript levels are not globally affected by cell density, pointing to a posttranscriptional mechanism underlying the increase in miRNA abundance under these conditions.

miRNA Accumulation with Increasing Cell Density Is Associated with Enhanced Drosha Processing Activity and Enhanced RISC Formation. Maturation of specific miRNAs has been demonstrated to be subject to regulation at the Dicer or Drosha processing steps (11, 12, 17, 26). We first evaluated these steps in miRNA biogenesis to assess their relative efficiencies in subconfluent and confluent cultures. The accumulation of both pre-miRNAs and mature miRNAs with increasing cell density (Fig. S1*B*) suggests that an increase in Dicer processing efficiency cannot account for the observed miRNA induction because this would be expected to increase mature miRNA abundance while decreasing pre-miRNA abundance. Furthermore, cells with impaired Dicer activity (27) exhibit prominent pre-miRNA accumulation with increasing confluency, demonstrating that the underlying mechanism is distinct from pre-miRNA processing (Fig. S3*A*). In vitro processing of a synthetic pre-miRNA confirms that extracts from confluent HeLa cells do not exhibit increased Dicer activity (Fig. S3*B*).

Next, we assessed whether the efficiency of Drosha processing is influenced by cell density. Four distinct in vitro-transcribed primary miRNA transcripts (miR-17, miR-21, miR-26a-2, and miR-29b-1) were incubated in extracts from subconfluent and confluent HeLa cells (Fig. 4*B* and Fig. S4). More efficient production of pre-miRNAs was consistently observed from all tested substrates in multiple independently derived extracts from confluent cells, indicating a general increase in Drosha processing efficiency. This was not because of higher expression of Drosha or its essential accessory factor DGCR8 in confluent cells, as demonstrated by Western blot analysis (Fig. S5*A*). These data demonstrate that increased Drosha processing activity contributes to the global increase in miRNA abundance that occurs with increasing cell density.

Although regulation of RISC formation or miRNA turnover has not previously been observed, we also considered the possibility that the kinetics of these aspects of miRNA biogenesis and metabolism are altered after cell–cell contact. To assess these processes, HeLa cells were transfected with a synthetic pre-miR-1 RNA oligonucleotide or an siRNA duplex targeting luciferase (si-Luc) and then plated at high or low density. Maturation of the pre-miR-1 oligo bypasses all steps upstream of Dicer processing, whereas si-Luc bypasses all steps upstream of RISC loading. Interestingly, both mature miR-1 and si-Luc exhibited higher abundance in confluent cultures (see total input lanes in Fig. 4*C*).
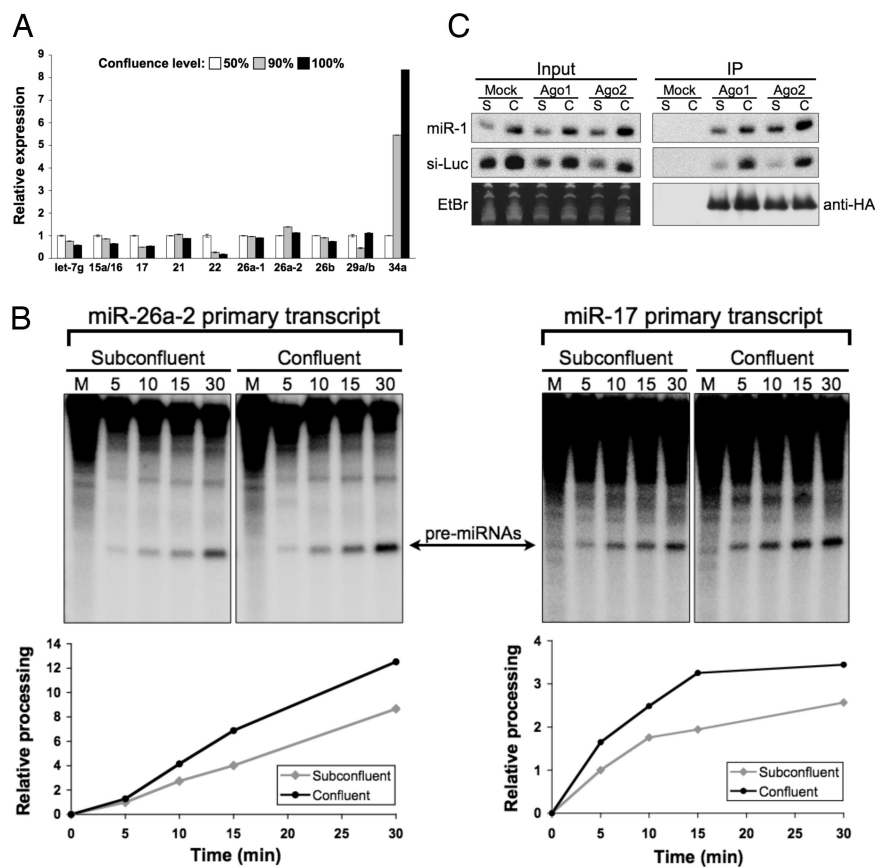
Fig. 3. Cell–cell contact likely triggers the global increase in miRNA abundance in confluent cultures. (*A*) miRNA abundance, cell number, and confluency were monitored daily during prolonged culture of HeLa cells. miRNA levels correlated with confluency despite no measurable reduction in cellular proliferation rate. (*B*) Increased miRNA abundance is not induced by cellular quiescence as demonstrated by unchanged or reduced expression of miRNAs in serum-starved subconfluent primary fibroblasts and NIH 3T3 cells (*Upper*). Propidium iodide staining and flow cytometry confirms efficient cell-cycle arrest after serum starvation (*Lower*). (*C*) Increased miRNA abundance is not triggered by diffusible factors, as demonstrated by unchanged or reduced expression of miRNAs in HeLa cells grown in media conditioned by subconfluent or confluent cells. (*D*) miRNAs do not accumulate significantly in high-density suspension cultures of Ramos or K562 cells.

These findings suggest that the final step in miRNA maturation, RISC formation, is enhanced, or miRNA turnover is reduced in cells grown to high density. Time-course studies after transfection of pre-miR-1 revealed no difference in the decay rate of mature miR-1 in subconfluent and confluent cells (Fig. S6). In contrast, immunoprecipitation experiments with HA-tagged Ago1 or Ago2 revealed greater incorporation of mature miR-1 into RISC in confluent cultures (Fig. 4C). Immunoprecipitation experiments with si-Luc similarly revealed greater incorporation of this siRNA into RISC at high cell density (Fig. 4C). These findings reveal an increase in the efficiency of RISC formation in confluent cells, identifying an additional regulated step in miRNA biogenesis that likely contributes to the increase in miRNA abundance after cell contact. Western blot analysis ruled out the possibility that this effect is due simply to increased abundance of Ago proteins, TRBP, or Exportin-5, factors that could potentially influence the kinetics of RISC formation (Fig. S5B).

Discussion

We have demonstrated that in diverse animal cell lines, the global efficiency of miRNA biogenesis is intimately linked to cell density. These findings reveal that careful monitoring of cellular confluency is critical for accurate analysis of miRNA expression and function in widely used cell culture systems and uncover an important caveat in the interpretation of earlier studies that did not closely monitor this parameter. Furthermore, these results provide insight into the cellular mechanisms that broadly influ-

ence miRNA expression patterns. For example, it is well documented that global miRNA abundance is generally higher in tissues compared with cell lines (19, 20). The widespread increase in miRNA abundance at high cell density likely contributes to this effect as both cells in tissues and confluent cells in culture elaborate extensive cell–cell contacts.

Our mechanistic studies have identified 2 posttranscriptional control points that link miRNA abundance to cell density. First, we find that Drosha processing efficiency is increased in confluent cells. Second, we show enhanced RISC formation under these conditions. Although the regulation of Drosha activity in other settings has been documented (11, 12, 14, 26), regulated RISC formation has not previously been observed. These findings are particularly interesting in light of accumulating evidence supporting a critical role for posttranscriptional mechanisms in the appropriate regulation of miRNA expression in normal physiologic states as well as in diseases such as cancer. During development, numerous primary miRNA transcripts are expressed but fail to be efficiently converted into the mature miRNA species (18). Moreover, tumors exhibit globally reduced miRNA levels due, at least in part, to decreased miRNA processing. The molecular mechanisms that control the global efficiency of miRNA biogenesis under these conditions remain largely uncharacterized, although some pathways that regulate maturation of specific miRNAs have recently been elucidated. For example, the Lin-28 RNA-binding protein has been shown to associate directly with let-7 family members during early embryonic development, preventing Drosha- and Dicer-mediated

Fig. 4. Increased Drosha processing activity and enhanced RISC formation contribute to the global increase in miRNA abundance in confluent cells. (*A*) Quantitative PCR demonstrating unchanged or decreased abundance of most miRNA primary transcripts in HeLa cells at increasing confluency. (*B*) In vitro Drosha processing assay demonstrating increased activity in extracts from confluent HeLa cells (M, mock; 5–30, length of reaction in minutes). Plots show the amount of pre-miRNA produced at each time point relative to the first time point in the subconfluent group. (*C*) Transfection with synthetic pre-miR-1 or si-Luc demonstrates enhanced RISC formation in confluent cells. HeLa cells were transfected with pre-miR-1 or si-Luc alone (Mock) or in combination with HA-tagged Ago1 or Ago2 expression plasmids and then plated at subconfluent (S) or confluent (C) densities. Northern blot analysis was used to assess mature miR-1 or si-Luc abundance in total lysate (Input) or anti-HA immunoprecipitates (IP). Representative ethidium bromide (EtBr)-stained gel demonstrates equal loading of total input. Western blot analysis using anti-HA antibody demonstrated approximately equal recovery of Ago proteins from subconfluent and confluent cells.

cleavage (11–15). Conversely, SMAD proteins recruit Drosha-containing complexes to miR-21 primary transcripts in vascular smooth muscle cells, enhancing processing (26). Given the broad nature of miRNA accumulation during late stages of development and, as shown here, at high cell density, it is unlikely that these highly specific mechanisms contribute to regulation of miRNA biogenesis in these settings. Rather, it is more plausible that Drosha-containing complexes and/or RISC-loading complexes are altered, either through association with accessory factors or by posttranslational modification, to elicit a general increase in mature miRNA production. Although these mechanisms await molecular definition, we note that our observations provide a tractable in vitro system for biochemical analysis of miRNA processing complexes under conditions where global miRNA biogenesis is regulated.

Materials and Methods

Cell Culture. HeLa, NIH 3T3, HEK293, MiaPaCa-2, Hepa1–6, and human primary fibroblast (CRL-2091; ATCC) cell lines were grown in Dulbecco's modified Eagle's medium. MCF7 cells were grown in minimum essential medium. HCT116 and HCT116-Dicer[ex5] cells were grown in McCoy's 5A medium. Ramos and K562 cells were grown in RPMI 1640 medium. All media for these cell lines was supplemented with 10% FBS. *Drosophila* S2R+ cells were grown in Schneider's *Drosophila* medium supplemented with 10% heat-inactivated FBS at room temperature. For measurements of miRNA abundance at various levels of confluency, media were replenished every day, and cell growth was monitored daily by counting. NIH 3T3 and HEK293 cells were grown on fibronectin-coated cultureware (BD Biosciences). Serum starvation experiments were performed by growing human primary fibroblasts in media containing 0.1% FBS for 48–96 h and NIH 3T3 cells in media without FBS for 48–72 h. To confirm cell-cycle arrest, cell-cycle profiles were analyzed after 48 h of serum starvation by propidium iodide (PI) staining in which cells were fixed in 70% ethanol overnight at −20 °C and then stained in 1× PBS containing 50 μg/mL PI and 100 μg/mL RNase A for 1 h at 4 °C. DNA content was then measured by flow cytometry. For media conditioning experiments (Fig. 3*C*), subconfluent HeLa cells were grown for 24 h in media transferred from dishes of subconfluent or confluent HeLa cells before isolation of RNA. For studying the

effects of cell density on miRNA accumulation in suspension cells (Fig. 3*D*), cells were seeded at various densities (K562: 0.5, 1, 2, and 4×10^6 per milliliter; Ramos: 0.25×10^6 per milliliter) and then allowed to grow for 24 h (K562) or 4 days (Ramos). Approximately 5×10^6 Ramos cells were harvested from the culture at 24-h intervals. Cell density was determined by hand counting using a hemocytometer before harvesting.

miRNA Expression Profiling. Custom microarrays containing oligonucleotide probes complementary to 474 human miRNAs were synthesized by Combimatrix. Array hybridization was performed as described (28). Signals <2 times the background level in both subconfluent and confluent cells were removed from analysis. Background-subtracted data are provided in Tables S1–S3.

Northern Blot Analysis. Northern blot analysis was performed as described (28, 29) by using Ultrahyb-Oligo buffer (Ambion) and oligonucleotide probes perfectly complementary to the mature miRNA sequences. All membranes were stripped and reprobed with appropriate loading controls (2S rRNA for *Drosophila* S2R+ cells and U6 snRNA or tRNA[Lys] for other cells).

Luciferase Assays. miR-15a and miR-143 luciferase reporter plasmids were constructed by ligating annealed oligonucleotides (sequences provided in Table S4) into the XbaI site of pGL3-control (Promega). Cloned sequences contained 2 perfectly complementary sites or 3 bulged sites with mismatches to nucleotide positions 9–12 of the corresponding miRNAs. Twenty-four hours before transfection, HeLa cells were plated at 20,000 and 150,000 per well of a 24-well plate. miRNA reporter plasmid (100 ng) along with 50 ng of renilla luciferase control plasmid (phRL-SV40; Promega) were transfected by using Lipofectamine 2000 (Invitrogen) according to the manufacturer's instructions. Luciferase assays were performed 24 h after transfection by using the Dual Luciferase Reporter Assay System (Promega). Each transfected well was assayed in triplicate. Firefly luciferase activity was normalized to renilla luciferase activity for each transfected well. Values were further normalized to luciferase activity produced by pGL3-control lacking miRNA-binding sites to control for nonspecific effects of the confluent or subconfluent state on luciferase expression. Assays were repeated 3 independent times on different days with multiple independent plasmid preparations.

Quantitative PCR. Total RNA was isolated by using TRIzol (Invitrogen) and further subjected to DNase I (Invitrogen) digestion. Reverse transcription was performed by using MMLV reverse transcriptase (Invitrogen) with random hexamer primers. Quantitative PCR was performed by using an ABI 7900 Sequence Detection System with the 2× SYBR green PCR master mix (Applied Biosystems). Each pri-miRNA was measured in triplicate. U6 snRNA abundance was used to normalize all values. Primer sequences are provided in Table S4 or were previously described (18, 30).

Western Blot Analysis. The following antibodies were used: rabbit polyclonal anti-TRBP (Abcam), rabbit polyclonal anti-Exportin 5 (Santa Cruz Biotechnology), rabbit polyclonal anti-DGCR8 (Proteintech Group Inc.), rabbit polyclonal anti-Drosha, mouse monoclonal anti-Ago family (Upstate Biotechnology), and mouse monoclonal anti-α-tubulin (Calbiochem).

In Vitro Processing Assays. *Construction of plasmids for production of in vitro-transcribed pri-miRNAs.* Fragments of the primary transcripts (pri-miRNAs) encoding miR-17 and miR-21 consisting of ≈80–150 bp of sequence flanking the miRNA hairpins were amplified from human genomic DNA and cloned into the XhoI (miR-17) or NheI (miR-21) sites of pcDNA3.1(+) (Invitrogen). Primer sequences are provided in Table S4. The pri-miR-26a-2 plasmid was constructed by subcloning the XhoI fragment containing the pri-miRNA from the previously described vector pMSCV-PIG-miR-26a-2 (28) into pcDNA3.1(+). The pri-miR-29b-1 plasmid was previously described (29). Sequences of all inserts were confirmed by direct sequencing.
Extract preparation. HeLa cells were plated at 1,875,000 cells per 15-cm dish and were grown for 1 or 4 days to achieve desired confluence levels (60–80% for subconfluent extracts, 100% for confluent extracts). To produce active extracts, 2×10^7 cells were harvested by scraping. After 2 washes with cold 1× PBS, cells were sonicated in buffer containing 20 mM Tris·HCl (pH 8.0), 100 mM KCl, and 0.2 mM EDTA and cleared by centrifugation. The total protein concentration of the extracts was determined by using the BCA assay (Thermo Scientific) and adjusted with lysis buffer if necessary to ensure equal total protein concentration between subconfluent and confluent extracts. In the cases where adjustment was needed, the confluent extracts always required dilution. Extracts were stored on ice, and assays were performed within 3 hours of cell lysis.
Drosha processing assays. Drosha processing assays were performed following the protocol by Lee and Kim (31). Radiolabeled pri-miRNAs were prepared by in vitro transcription of XbaI-linearized plasmids with [α-^{32}P]UTP by using the MAXIscript kit (Ambion) followed by gel purification, phenol-chloroform extraction and ethanol precipitation. Processing reactions consisted of 15 μL of cell extract, 3 μL of 64 mM MgCl$_2$, 2 μL of radiolabeled pri-miRNA (≈1 × 10^5 cpm), 1 μL of RNaseOUT (Invitrogen), and 9 μL of DEPC water. Reactions were incubated at 37 °C. At each time point, reactions were stopped by adding phenol-chloroform and vortexing vigorously. Mock reactions were performed exactly as described above except lysis buffer was added in lieu of cell extract.
Dicer processing assays. Dicer processing assays were performed as above with the following modifications: The processing substrate consisted of an RNA oligo identical in sequence to human pre-miR-199b (obtained from Dharmacon; se-

quence provided in Table S4), which was end-labeled with [γ-^{32}P]ATP by using T4 polynucleotide kinase (New England Biolabs). Processing reactions consisted of 15 μL of extract, 2 μL of 64 mM MgCl$_2$, 1 μL of radiolabeled pre-miRNA (≈1 × 10^5 cpm), 1.5 μL of RNaseOUT (Invitrogen), and 10.5 μL of DEPC water.
Analysis. All reactions were phenol-chloroform extracted and ethanol precipitated and then separated on a 12% denaturing polyacrylamide gel. Images were obtained by exposing the gel to a phosphor screen overnight. Image acquisition and analysis were performed by using Quantity One software (Bio-Rad).

RISC Formation Analysis. To investigate effects of cell density on RISC formation (Fig. 4C), 2×10^6 HeLa cells were plated per 10-cm dish in media containing no antibiotics. The next day, cells were transfected with 10 nM pre-miR-1 oligo or Luc siRNA (obtained from Dharmacon; sequences provided in Table S4) alone or with 8 μg of Flag/HA-tagged human Ago1 or Ago2 (32). Transfection was performed by using Lipofectamine 2000 (Invitrogen) according to manufacturer's instructions. The next day, transfected cells were pooled and replated at the desired confluence levels (ensuring that the transfection efficiency was the same for both confluent and subconfluent conditions). HeLa cells (4.8×10^6 or 1.8×10^6) were plated respectively per 10-cm dish or 6-cm dish for the confluent group (95≈100% confluent the next day) whereas 0.6×10^6 cells were plated per 10-cm dish for the subconfluent group (50≈60% confluent the next day).

Twenty-four hours after replating, cells were counted, washed with cold 1× PBS twice, collected by scraping, and then lysed in buffer containing 50 mM Tris·HCl (pH 7.5), 150 mM NaCl, 2 mM MgCl$_2$, 2 mM CaCl$_2$, 1 mM DTT, 0.5% Nonidet-40, and complete mini EDTA-free protease inhibitor mixture (Roche Applied Science). For each group, the lysate was made from 5 to 8×10^6 cells. The lysate was incubated on ice for 10 min with occasional mixing to complete lysis and then centrifuged at $12,000 \times g$ for 10 min at 4 °C to remove nuclear pellets. After centrifugation, the lysates were rotated with 4–6 μg of anti-HA mouse monoclonal antibody (Covance) for 1 h at 4 °C. Immunoprecipitation of Flag/HA-tagged human Ago1 and Ago2 was performed by rotating the lysates for additional 3 h at 4 °C after adding 100 μL of a 50% slurry of protein G-agarose beads (Roche Applied Science). The beads were harvested by centrifugation and washed 6 times in lysis buffer. Eighty percent of the beads were resuspended in 1 mL of TRIzol for RNA isolation and 20% of the beads were resuspended in 20 μL of 2× complete Laemmli buffer for protein analysis.

Concurrently, stability of mature miR-1 at confluent and subconfluent states was assayed by harvesting confluent and subconfluent HeLa cells at various time points beginning 24 h after replating. For each time point, cytoplasmic lysates from 1 6-cm dish of confluent and 2 10-cm dishes of subconfluent HeLa cells were prepared as above. The lysates were then added to 1–2 mL of TRIzol for RNA isolation.

CELL BIOLOGY

1. Bartel DP (2004) MicroRNAs: Genomics, biogenesis, mechanism, and function. *Cell* 116:281–297.
2. Zamore PD, Haley B (2005) Ribo-gnome: The big world of small RNAs. *Science* 309:1519–1524.
3. Kim VN (2005) MicroRNA biogenesis: Coordinated cropping and dicing. *Nat Rev Mol Cell Biol* 6:376–385.
4. Valencia-Sanchez MA, Liu J, Hannon GJ, Parker R (2006) Control of translation and mRNA degradation by miRNAs and siRNAs. *Genes Dev* 20:515–524.
5. Kloosterman WP, Plasterk RH (2006) The diverse functions of microRNAs in animal development and disease. *Dev Cell* 11:441–450.
6. Ambros V (2004) The functions of animal microRNAs. *Nature* 431:350–355.
7. Wienholds E, et al. (2005) MicroRNA expression in zebrafish embryonic development. *Science* 309:310–311.
8. Thomson JM, Parker J, Perou CM, Hammond SM (2004) A custom microarray platform for analysis of microRNA gene expression. *Nat Methods* 1:47–53.
9. Liu N, et al. (2007) An intragenic MEF2-dependent enhancer directs muscle-specific expression of microRNAs 1 and 133. *Proc Natl Acad Sci USA* 104:20844–20849.
10. Zhao Y, Samal E, Srivastava D (2005) Serum response factor regulates a muscle-specific microRNA that targets Hand2 during cardiogenesis. *Nature* 436:214–220.
11. Viswanathan SR, Daley GQ, Gregory RI (2008) Selective blockade of microRNA processing by Lin28. *Science* 320:97–100.
12. Newman MA, Thomson JM, Hammond SM (2008) Lin-28 interaction with the Let-7 precursor loop mediates regulated microRNA processing. *RNA* 14:1539–1549.
13. Rybak A, et al. (2008) A feedback loop comprising lin-28 and let-7 controls pre-let-7 maturation during neural stem-cell commitment. *Nat Cell Biol* 10:987–993.
14. Piskounova E, et al. (2008) Determinants of microRNA processing inhibition by the developmentally regulated RNA-binding protein Lin28. *J Biol Chem* 283:21310–21314.
15. Heo I, et al. (2008) Lin28 mediates the terminal uridylation of let-7 precursor MicroRNA. *Mol Cell* 32:276–284.
16. Lee EJ, et al. (2008) Systematic evaluation of microRNA processing patterns in tissues, cell lines, and tumors. *RNA* 14:35–42.
17. Obernosterer G, Leuschner PJ, Alenius M, Martinez J (2006) Post-transcriptional regulation of microRNA expression. *RNA* 12:1161–1167.
18. Thomson JM, et al. (2006) Extensive post-transcriptional regulation of microRNAs and its implications for cancer. *Genes Dev* 20:2202–2207.
19. Gaur A, et al. (2007) Characterization of microRNA expression levels and their biological correlates in human cancer cell lines. *Cancer Res* 67:2456–2468.
20. Lu J, et al. (2005) MicroRNA expression profiles classify human cancers. *Nature* 435:834–838.
21. Kumar MS, Lu J, Mercer KL, Golub TR, Jacks T (2007) Impaired microRNA processing enhances cellular transformation and tumorigenesis. *Nat Genet* 39:673–677.
22. Abercrombie M (1979) Contact inhibition and malignancy. *Nature* 281:259–262.
23. Johnson KC, Kissil JL, Fry JL, Jacks T (2002) Cellular transformation by a FERM domain mutant of the Nf2 tumor suppressor gene. *Oncogene* 21:5990–5997.
24. Wu Y, et al. (2001) Overexpression of Hp95 induces G$_1$ phase arrest in confluent HeLa cells. *Differentiation* 67:139–153.
25. He L, He X, Lowe SW, Hannon GJ (2007) microRNAs join the p53 network—another piece in the tumour-suppression puzzle. *Nat Rev Cancer* 7:819–822.
26. Davis BN, Hilyard AC, Lagna G, Hata A (2008) SMAD proteins control DROSHA-mediated microRNA maturation. *Nature* 454:56–61.
27. Cummins JM, et al. (2006) The colorectal microRNAome. *Proc Natl Acad Sci USA* 103:3687–3692.
28. Chang TC, et al. (2008) Widespread microRNA repression by Myc contributes to tumorigenesis. *Nat Genet* 40:43–50.
29. Hwang HW, Wentzel EA, Mendell JT (2007) A hexanucleotide element directs microRNA nuclear import. *Science* 315:97–100.
30. O'Donnell KA, Wentzel EA, Zeller KI, Dang CV, Mendell JT (2005) c-Myc-regulated microRNAs modulate E2F1 expression. *Nature* 435:839–843.
31. Lee Y, Kim VN (2007) In vitro and in vivo assays for the activity of Drosha complex. *Methods Enzymol* 427:89–106.
32. Meister G, et al. (2004) Human Argonaute2 mediates RNA cleavage targeted by miRNAs and siRNAs. *Mol Cell* 15:185–197.